

Supporting information for: **Inverted organic photovoltaics with a solution-processed Mg-doped ZnO electron transport layer annealed at 150 °C**

Ioannis Ierides^a, Giovanni Ligorio^b, Martyn A. McLachlan^c, Kunping Guo^a, Emil J. W. List-Kratochvil^{b,d} and Franco Cacialli^{*a}

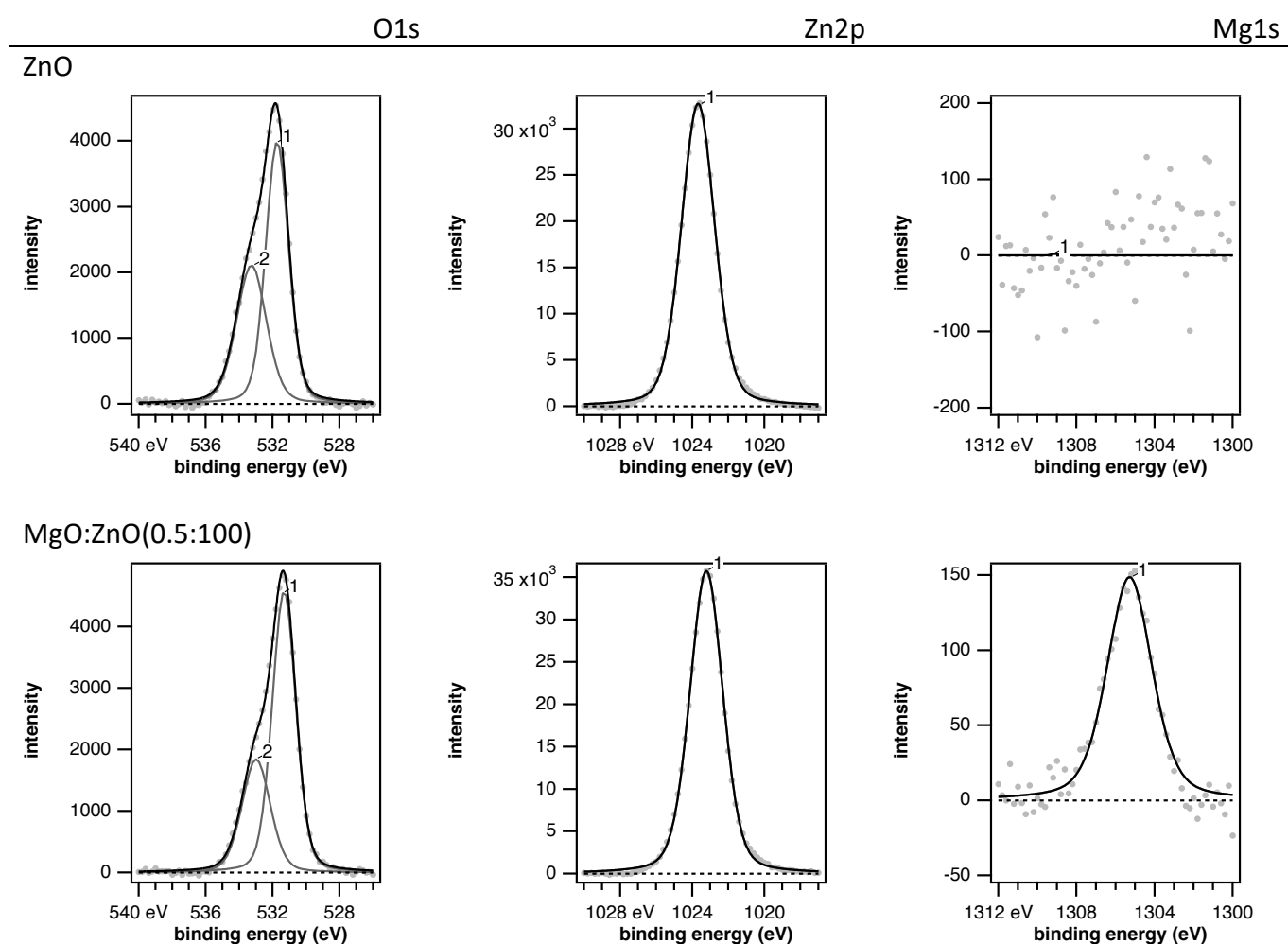
^aDepartment of Physics and Astronomy and London Centre for Nanotechnology, University College London, London, WC1E 6BT, United Kingdom

^bInstitut für Physik, Institut für Chemie & IRIS Adlershof, Humboldt-Universität zu Berlin, Zum Großen Windkanal 2, 12489 Berlin, Germany

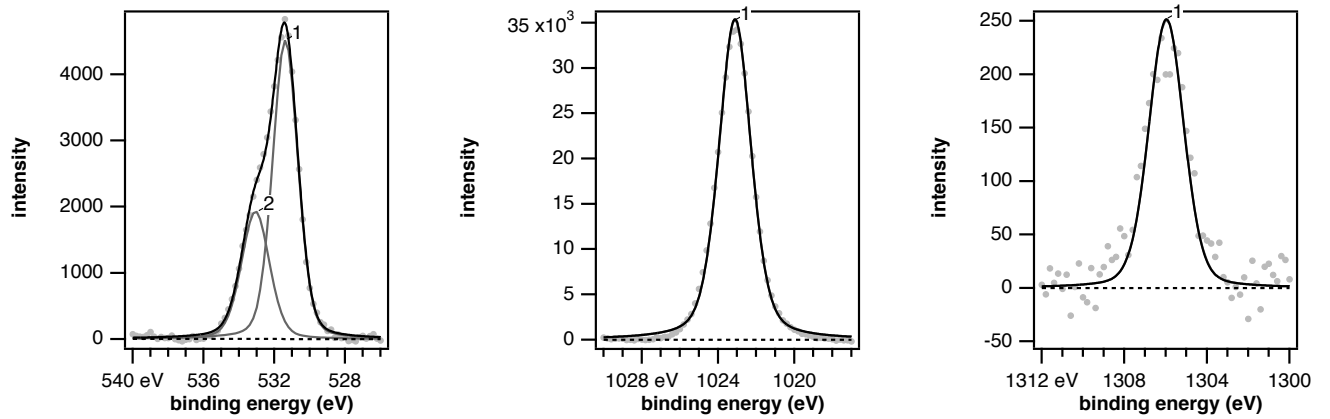
^cDepartment of Materials and Centre for Processable Electronics, Imperial College London, London SW7 2AZ, UK

^dHelmholtz-Zentrum Berlin für Materialien und Energie GmbH, Hahn-Meitner-Platz 1, 14109 Berlin, Germany

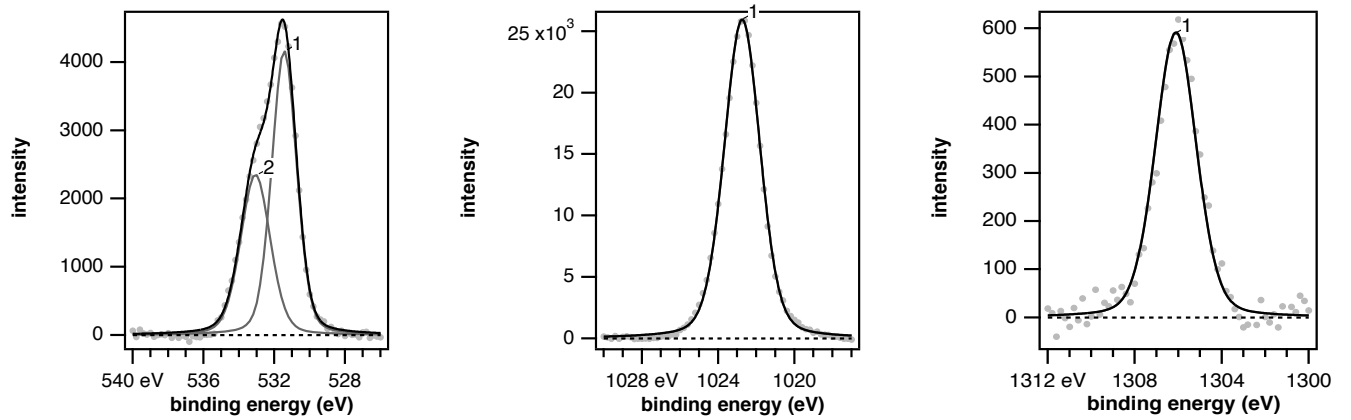
x-ray photoelectron spectroscopy (XPS) data



MgO:ZnO(1:100)



MgO:ZnO(3:100)



MgO:ZnO(5:100)

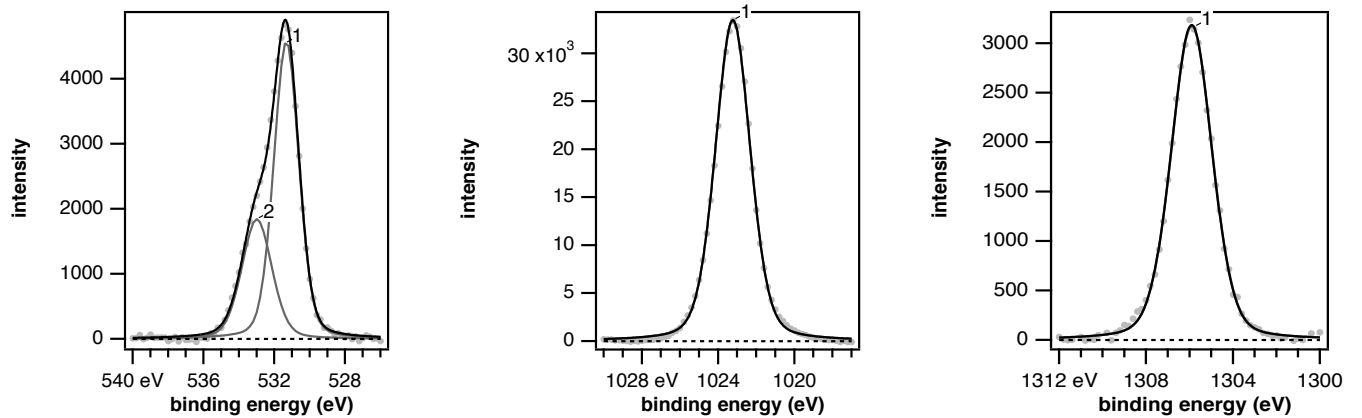


Fig S1: The O1s, Zn2p and Mg1s core level signals collected via XPS of ETLs with different Mg doping concentrations. The scattered data points report the spectra upon background correction (the Shirley function was subtracted). The lines are the best fits employing Voigt functions.

ETL (MgO:ZnO)	Zn2p (%)	Mg1s (%)	C1s (%)	O1s (%)
ZnO	38.2	0	15.1	46.7
(0.5:100)	40.3	0.4	11.6	47.8
(1:100)	38.6	0.5	12.6	48.3
(3:100)	37.7	1.1	12.3	48.8
(5:100)	34.9	1.9	13.2	50

Table S1: Relative concentration of the number of atoms for the atomic species found in the various Mg-doped films as measured by XPS.

EQE (J_{SC} extraction) of PTB7-Th:PC₇₀BM (fullerene based) OPVs presented in Figure 1

ETL (MgO:ZnO)	J_{SC} experimental (mAcm⁻²)	J_{SC} calculated (mAcm⁻²)
ZnO	8.46 ± 0.04	8.36 ± 0.09
(1:100)	9.05 ± 0.04	9.01 ± 0.09
(5:100)	8.44 ± 0.04	8.34 ± 0.09

Table S2: Extracted J_{SC} from integrating the EQE spectra of devices using the typical 1 sun spectrum. The calculated J_{SC} matches the J_{SC} measured by the photovoltaic characterisation.

Performance of Mg-doped ZnO based OPVs for PM6:Y6 (non-fullerene acceptor) active layers

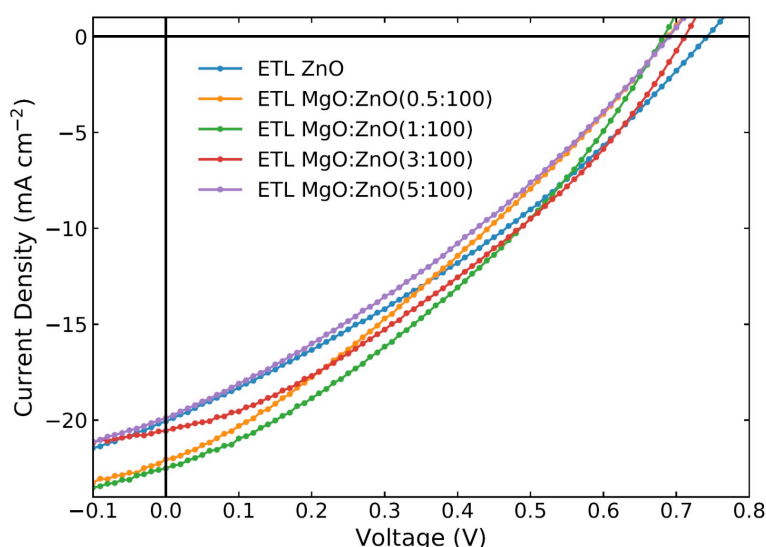


Fig S2: Representative current density vs. voltage curves under 1 sun for OPV devices based on a PM6:Y6 active layer with ETLs containing various Mg doping levels.

ETL (MgO:ZnO)	PCE (%)	J_{SC} (mAcm ⁻²)	V_{OC} (mV)	FF
ZnO	5.21 ± 0.53	20.74 ± 0.48	737 ± 35	0.34 ± 0.02
(0.5:100)	5.09 ± 0.53	21.97 ± 0.48	704 ± 35	0.33 ± 0.02
(1:100)	5.48 ± 0.53	22.21 ± 0.48	688 ± 35	0.36 ± 0.02
(3:100)	5.36 ± 0.53	20.91 ± 0.48	693 ± 35	0.37 ± 0.02
(5:100)	4.93 ± 0.53	19.97 ± 0.48	710 ± 35	0.35 ± 0.02

Table S3: Extracted parameters for OPV devices presented in Figure S2.

ETL (MgO:ZnO)	J_{SC} experimental (mAcm ⁻²)	J_{SC} calculated (mAcm ⁻²)
ZnO	20.74 ± 0.48	19.8 ± 1.0
(1:100)	22.21 ± 0.48	22.3 ± 1.0
(5:100)	19.97 ± 0.48	19.7 ± 1.0

Table S4: Extracted J_{SC} from integrating the EQE spectra of devices using the typical 1 sun spectrum. The calculated J_{SC} matches the J_{SC} measured by the photovoltaic characterisation.

The above findings demonstrate that the use of Mg-doped ZnO ETLs is also beneficial to PM6:Y6 OPVs and thus not confined to fullerene-acceptors OPVs. The trends observed here are similar to those of the PTB7-Th:PC₇₀BM devices in terms of J_{SC} and the FF. The V_{OC} of the measured devices (for each type of ETL) varied significantly, leading to a large uncertainty in V_{OC} and preventing solid conclusions regarding the V_{OC} trend. Nevertheless, in terms of PCE and similarly to the PTB7-Th:PC₇₀BM OPVs, the best performing devices are the ones that employ an Mg-doped ZnO ETL formed from a MgO:ZnO precursor ratio of 1:100, yielding a PCE ~ 5.48 ± 0.53. For this type of active layer the maximum relative increase in PCE is ~5% with respect to the device employing the undoped ZnO ETL. This is lower than the one observed with PTB7-Th:PC₇₀BM devices, but still significant.

Comparison of PV performance for different annealing temperatures

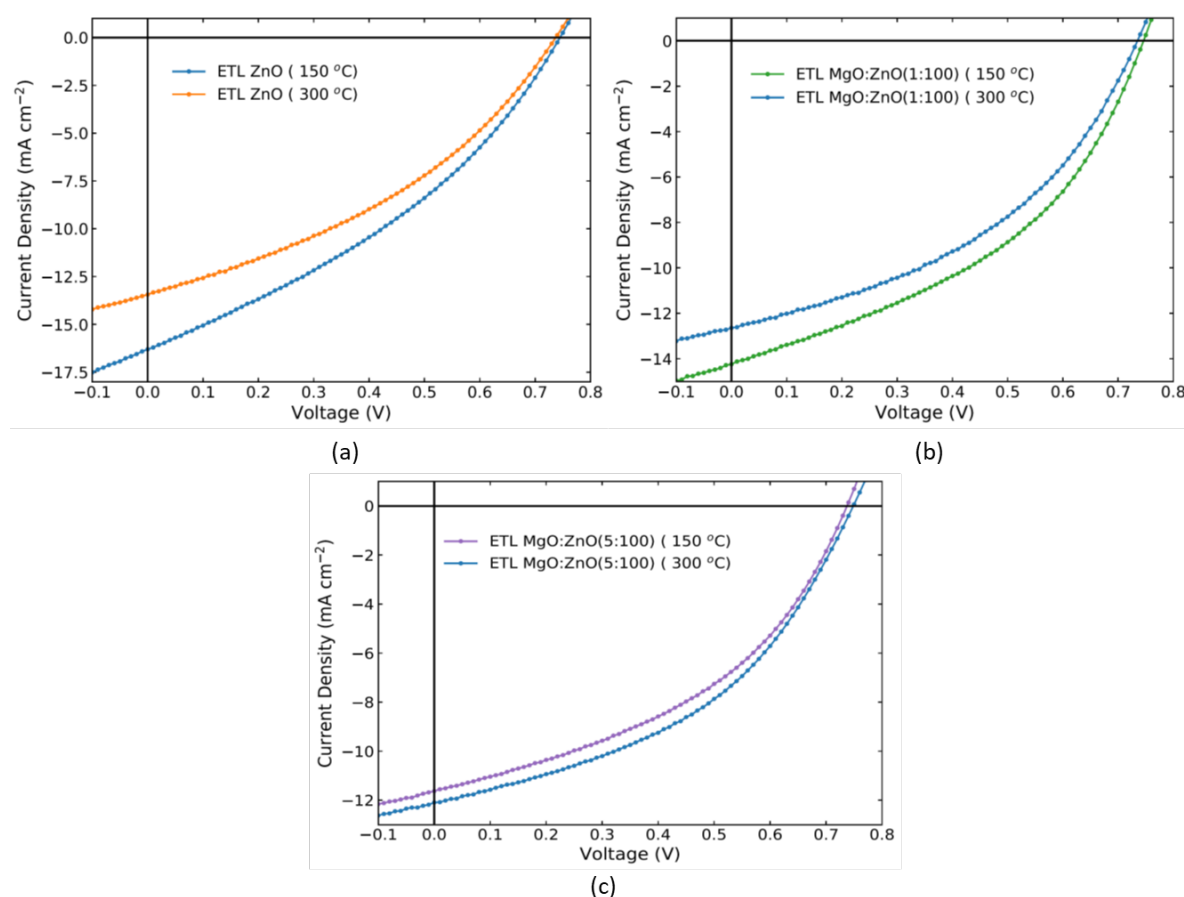


Fig S3: Representative current density vs. voltage curves under 1 sun comparing OPVs with the ETL annealed at temperatures of 150 °C vs 300 °C for (a) ZnO-only ETLs, and ETLs formed from MgO:ZnO precursor ratios of (b) 1:100 and (c) 5:100.

ETL (MgO:ZnO) (Annealing temperature)	PCE (%)	J _{sc} (mAcm ⁻²)	V _{oc} (mV)	FF
ZnO (150°C)	4.26 ± 0.13	15.98 ± 0.72	747 ± 4	0.36 ± 0.01
ZnO (300°C)	4.00 ± 0.13	13.86 ± 0.72	741 ± 4	0.39 ± 0.01
(100:1) (150°C)	4.37 ± 0.13	14.48 ± 0.72	745 ± 4	0.41 ± 0.01
(100:1) (300°C)	3.73 ± 0.13	12.62 ± 0.72	734 ± 4	0.40 ± 0.01
(100:5) (150°C)	3.58 ± 0.13	11.62 ± 0.72	736 ± 4	0.42 ± 0.01
(100:5) (300°C)	3.77 ± 0.13	12.05 ± 0.72	745 ± 4	0.42 ± 0.01

Table S5: Extracted parameters for OPV devices presented in Figure S3.

The findings above suggest that the ETL Mg loading required to maximise the PCE depends on the ETL annealing temperature. For the key temperature of 150 °C (that enables compatibility with the flexible substrates) the optimum loading is 1-3%. However, at 300 °C this is no longer the optimum loading. This finding is in line with previous reports in the literature^{1,2} (that employ annealing temperatures of 300 °C or so) where a much higher Mg-loading is required to achieve optimised performance. It is also useful to note that for the undoped ZnO ETL and the ETL formed from a MgO:ZnO precursor ratio 1:100 (that shows the highest performance) annealing at 150 °C rather than 300 °C yields devices with higher PCE.

The increase in efficiency when comparing the PCE of the undoped ZnO ETL and the ETL formed from a MgO:ZnO precursor ratio of 1:100 annealed at 150 °C for this new batch tested, differs from the 18% reported in the manuscript in terms of absolute value, however the overall efficiency trend between the different Mg doping amounts is consistent.

Determining the correlation between temperature and Mg loading required to optimise the PCE of OPVs is beyond the scope of this paper. In the following paragraph, we provide some speculative statements regarding the potential mechanisms behind the findings presented above, noting that a more exhaustive study would be required to confirm these considerations.

The annealing temperature might play a significant role in determining the optimum Mg loading for Mg-doped ZnO ETLs due to the degree of decomposition of the zinc and magnesium acetate precursors achieved at different temperatures. At 300 °C crystalline ZnO starts to form, hence the presence of only a limited amount of Mg might hinder crystallinity and thus performance, whereas much higher Mg doping might lead to a favourable crystalline structure. In addition, much higher levels of Mg (than in the range tested in the manuscript) have been shown to affect other characteristics of the films (such as its work function, bandgap, mobility, etc.) and the different balance of all these factors leads to the necessity of a different (and higher) Mg loading to achieve an increase in performance via Mg doping at 300 °C. At 150 °C the acetates do not decompose fully, and the benefit of limited Mg addition is likely to be related to the filling of oxygen vacancies with optimisation achieved in the doping range of 1-3%. Higher doping percentages for this temperature regime may hinder performance due to an overcompensation of the oxygen vacancies.

Ultraviolet photoelectron spectroscopy (UPS) :

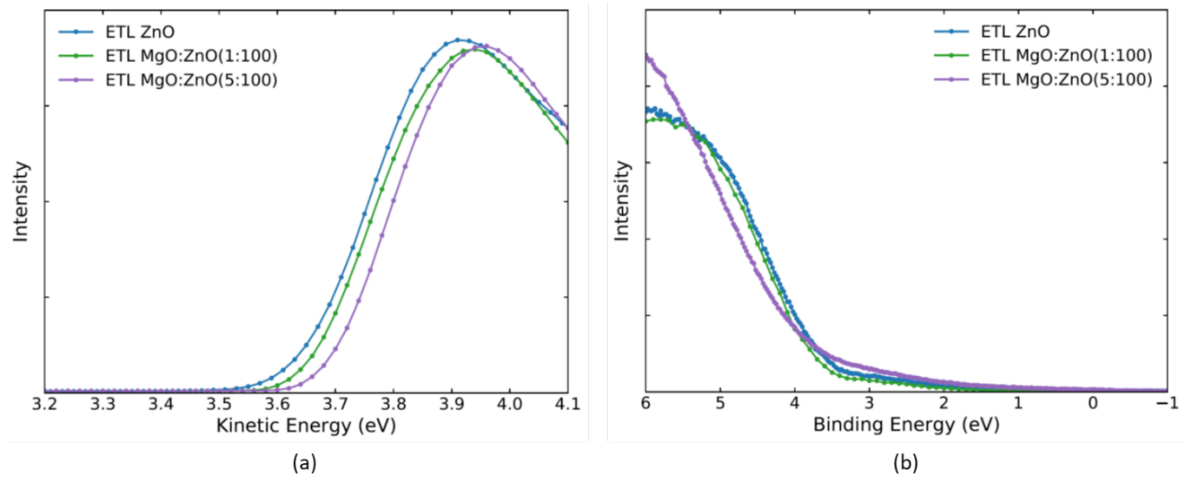


Fig S4: (a) The secondary electron cut-off spectra and (b) the valence band region spectra collected with UPS.

Optical transmittance

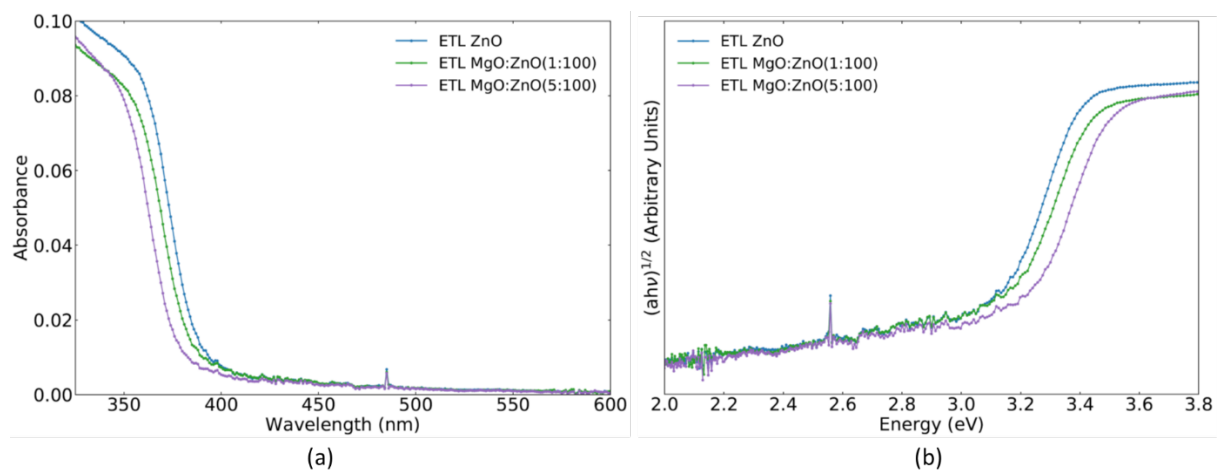


Fig S5: (a) Transmittance spectra presented in the form of Absorbance (not corrected for reflectance). (b) Corresponding Tauc plots (α =absorption coefficient).

The results in Figure S5 show that potential changes in energetics are of the order of 0.1 eV or so (equivalent to the uncertainty on UPS and Kelvin probe measurements). The above findings corroborate that for the minimal Mg doping used in these investigations no significant changes in the energetics of the devices are observed.

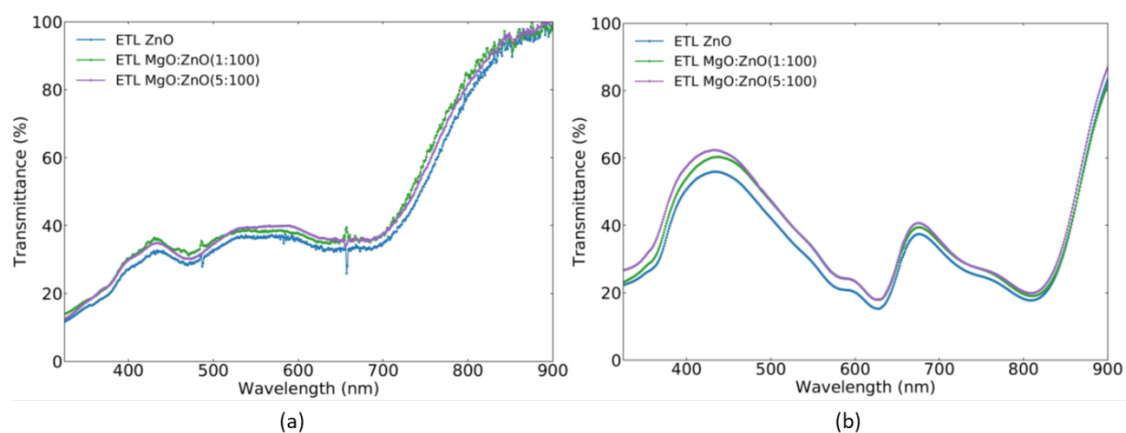


Fig S6: (a) Transmission spectra of ITO/ZnO/PTB7-Th:PC₇₀BM, ITO/Mg-doped (1:100) ZnO/PTB7-Th:PC₇₀BM and ITO/Mg-doped (5:100) ZnO/PTB7-Th:PC₇₀BM films. (b) Transmission spectra of ITO/ZnO/PM6:Y6, ITO/Mg-doped (1:100) ZnO/PM6:Y6 and ITO/Mg-doped (5:100) ZnO/PM6:Y6 films. The Mg-doped ZnO films show a slightly higher transmittance.

Electrical characterisation of Mg-doped ZnO (PM6:Y6) non-fullerene acceptor OPV devices

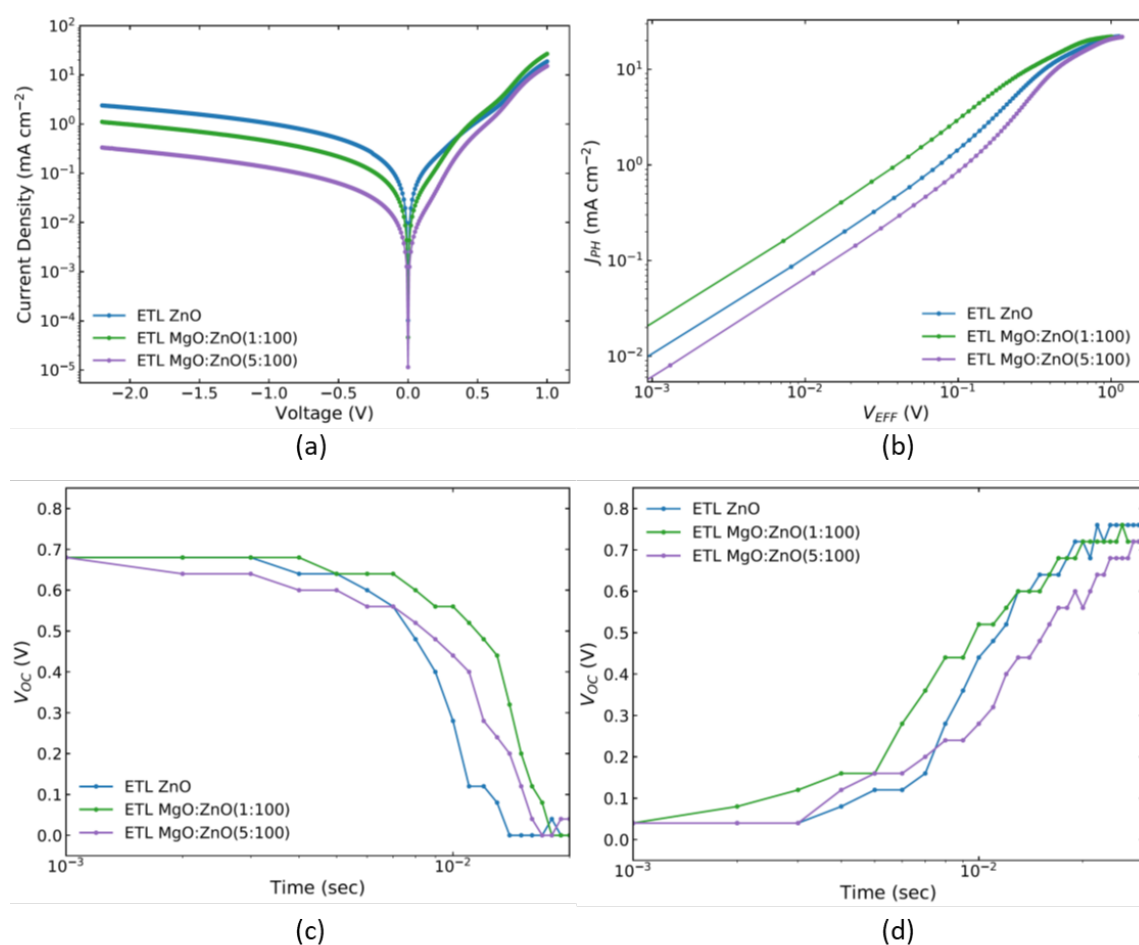


Fig S7: (a) Current density–voltage curves in the dark. (b) Photocurrent density - effective voltage curves. (c) Open circuit voltage decay curves (in the dark). (d) Open circuit voltage rise curves (under 1 sun).

ETL (MgO:ZnO)	J_{DARK} at -1V (mAcm ⁻²)	R_{sh} (Ω cm ²)
ZnO	- 1.04	1142
(1:100)	-0.50	2650
(5:100)	-0.18	6192

Table S6: The average current density at -1 V and resulting R_{sh} values for the PM6:Y6 OPV devices.

Similarly to the PTB7-Th:PC₇₀BM devices, the incremental addition of Mg in the ZnO ETL leads to a reduction in the current leakage and a corresponding increase in the shunt resistance.

Equivalent circuit of organic photovoltaic devices in the dark

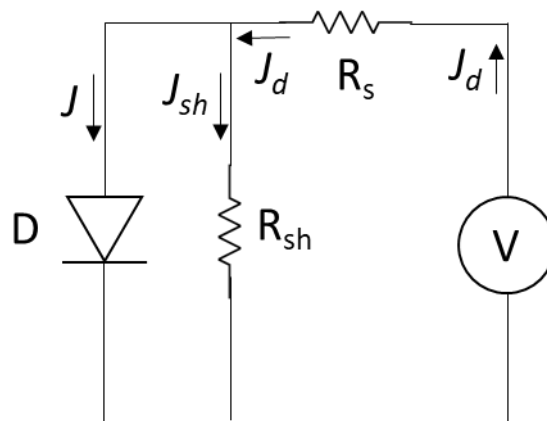


Fig S8: The equivalent circuit used to model organic photovoltaic devices when operated in the dark. An increased shunt resistance (R_{sh}) leads to a reduction in the leakage (reverse bias) current of the devices.

References

1. Z. Yin, Q. Zheng, S. C. Chen, D. Cai, L. Zhou and J. Zhang, *Adv. Energy Mater.*, 2014, 4, 1301404.
2. B. A. MacLeod, P. Schulz, S. R. Cowan, A. Garcia, D. S. Ginley, A. Kahn and D. C. Olson, *Adv. Energy Mater.*, 2014, 4, 1400073.